

# Three-dimensional reconstructions from low-count SPECT data using deformable models with smooth interior intensity variations

G. S. Cunningham and K. M. Hanson

*MS P940, Los Alamos National Laboratory, Los Alamos, NM 87545 USA*

*cunning@lanl.gov and kmh@lanl.gov*

**Abstract:** We demonstrate the reconstruction of a 3D, time-varying bolus of radiotracer from first-pass data obtained by the dynamic SPECT imager, FASTSPECT, built by the University of Arizona. The object imaged is a CardioWest Total Artificial Heart. The bolus is entirely contained in one ventricle and its associated inlet and outlet tubes. The model for the radiotracer distribution is a time-varying triangulated surface with voxel-to-voxel variations allowed inside the volume defined by the closed surface. The total curvature of the surface as well as the point-to-point variation of the interior voxel values is minimized through the use of weighted priors in the Bayesian framework. MAP estimates for the vertices, voxel values, and background count levels are produced for a subset of the 100 available 50-msec frames. The strengths of the priors (the hyperparameters) are determined by maximizing the evidence for the data over the hyperparameter values under the assumption that the posterior is approximately Gaussian.

---

## References

1. W. P. Klein, H.H. Barrett, I. W. Pang, D. D. Patton, M. M. Rogulski, J. J. Sain, and W. Smith "FASTSPECT: Electrical and mechanical design of a high resolution dynamic SPECT imager," *Conference Record of the 1995 IEEE Nucl. Sci. Symp. & Med. Imaging Conf.*, vol. 2, pp. 931-933 (IEEE, Los Alamitos, 1996).
2. G. S. Cunningham, K. M. Hanson, and X. L. Battle, "Three-dimensional reconstructions from low-count SPECT data using deformable models" *Optics Express* **2** (6), pp. 227-236 (1998) (available online at <http://epubs.osa.org/opticsexpress>).
3. X.L. Battle, G. S. Cunningham, and K. M. Hanson, "Tomographic reconstruction using 3D deformable models," *Phys. Med. Biol.* **43**, pp 983-990 (1998).
4. K. M. Hanson, R. L. Bilisoly, and G. S. Cunningham, "Kinky tomographic reconstruction," *Proc. SPIE* **2710**, pp. 156-166 (SPIE, Bellingham, 1996).
5. D. J. C. MacKay, "Bayesian interpolation," *Neural Comput.* **4**, pp. 415-447 (1992).
6. P. C. Hansen and D. P. O'Leary, "The use of the L-curve in the regularization of discrete ill-posed problems," *SIAM J. Sci. Comput.* **14**, pp. 1487-1503 (1993).
7. Z. Bai, M. Fahey, and G. Golub, "Some large-scale matrix computation problems," *J. Comp. App. Math.* **74**, pp. 71-89 (1996).

---

## 1. Introduction

The FASTSPECT imaging system [1], developed at the University of Arizona, has been used for first-pass tomographic imaging of the time-varying distribution of a bolus of Tc-99m pertechnetate radiotracer infused into a CardioWest Total Artificial Heart. The FASTSPECT machine simultaneously provides 24 pinhole views of the bolus distribution evolving in time, and is unique in its ability to perform this type of dynamic imaging. The goal in obtaining first-pass tomographic data is to demonstrate that clinically important measures of heart function, such as ejection fraction and wall motion, can be quantitatively estimated without having to gate and average over many cardiac cycles, an approach necessarily utilized by

single- or dual-head cardiac SPECT systems. If ejection fraction and wall motion can be estimated from first-pass data during the first few cardiac cycles, then later cycles can be used to estimate myocardial perfusion, another important indicator of heart function. If successful, the FASTSPECT approach would mean that a single, relatively cheap instrument could perform multiple diagnostic tests of cardiac function with a single bolus of radiotracer. This type of capability would be clinically valuable and affordable for use in emergency rooms across the country to do initial assessment of cardiac patients.

A traditional approach to reconstruction of the 24-view tomographic data might employ the EM method to produce the maximum likelihood estimate of the activity in each voxel of the volume being imaged. The voxel data could then be segmented to yield an estimate of an isosurface of the radiotracer distribution. Surface estimates performed in this way will be unacceptably noisy for the type of data analyzed in this article. For such sparse and noisy data, an approach that directly estimates the shape parameters of a time-varying surface from the raw projection data is advantageous, although potentially very time-consuming.

In previous work [2,3], we discussed the direct estimation approach and applied it to real data obtained by FASTSPECT. In that work, we formulated a Bayesian estimation problem for first-pass tomographic imaging using FASTSPECT that directly estimated the time-varying

$(x, y, z)$  components of the vertices of a triangulated surface within which it was assumed that the bolus was uniformly distributed. The estimation was performed by doing a quasi-Newton minimization of the minus-log posterior over the large-dimensional parameter space. The computation time associated with the direct estimation approach was argued to be comparable to the time required by the traditional approach, due to the fact that we utilized the adjoint differentiation technique to compute search directions needed by the optimization.

We have made several improvements to the techniques described in our previous work. First, we have relaxed the assumption that the intensity of the volume interior to the triangulated surface is uniform. We now allow the intensity to vary on a voxel-to-voxel basis, but penalize the square of the norm of the numerical gradient of the voxels inside the surface. This new model encourages smoothness of the inhomogeneous intensity distribution within the surface while still allowing for sharp discontinuities in intensity across the surface boundary. Second, smoothness of the surface is now relaxed at the tube/ventricle join, which allows the surface to model the physically realistic high-curvature connection between the tube and the ventricle. This region is manually labeled by the user of the analysis program by simply placing a sphere in the neighborhood of the surface where high curvature is to be allowed. Finally, in our current approach, we obtain the optimal values of the hyperparameters for the two smoothness priors by computing the evidence for the data as a function of the hyperparameters, and selecting the values that yield the maximum evidence.

## 2. Recent improvements in the direct estimation approach

### 2.1 The Bayesian estimation problem

The Bayesian estimation problem is to find the values for the surface parameters,  $\mathbf{x}_1$ , voxel values,  $\mathbf{x}_2$ , and background count level,  $s$ , that produce the maximum *a posteriori* (MAP) probability, or the minimum minus-log posterior:

$$\mathbf{x}^{\text{MAP}}(\alpha, \beta) = \arg \min_{\mathbf{x}} [\phi(\mathbf{x}_1, \mathbf{x}_2, s) + \alpha \pi_1(\mathbf{x}_1) + \beta \pi_2(\mathbf{x}_2)], \quad (3)$$

where  $\mathbf{x}$  is a concatenation of  $\mathbf{x}_1$  and  $\mathbf{x}_2$ ,  $\phi(\mathbf{x}_1, \mathbf{x}_2, s)$  is the minus log probability of the data given the parameters, and the next two terms are the minus log prior probabilities for the surface and voxel parameters, respectively, for some fixed value of the hyperparameters,  $\alpha$  and  $\beta$ . The higher-order problem is to determine  $\alpha$  and  $\beta$  from the data. The Bayesian solution to the higher-order problem is to determine the  $\alpha$  and  $\beta$  that yield the greatest evidence for the data, where the evidence is the integral w.r.t. parameters over the joint

posterior distribution of parameters and data (leaving just the probability of the data given the hyperparameters, called the evidence) [5].

In our previous work, we determined  $\alpha$  using the L-curve [6], the continuum of 2D points,

$$(\phi(\mathbf{x}^{\text{MAP}}(\alpha)), \pi(\mathbf{x}^{\text{MAP}}(\alpha))), \quad (4)$$

parameterized by  $\alpha$ . The value of  $\alpha$  chosen for the final estimate was the one that yielded the point on the L-curve that was closest to the “corner”. Due to the ad hoc nature of the L-curve criterion, and the vagueness of what is meant by “corner”, we now calculate the evidence assuming that the posterior is approximately Gaussian. However, calculating the evidence is very costly, since one must evaluate the determinant of a large, sparse, matrix for all values of  $\alpha$  and  $\beta$ .

## 2.2 Introduction of smooth inhomogeneities

In our previous work, the intensity of the radiotracer interior to the triangulated surface was assumed to be constant. However, this model is obviously inaccurate to some degree, and so we have explored the utility of allowing voxel-to-voxel variations within the volume defined by the surface. The voxel-to-voxel variations are penalized by the prior,  $\pi_2$ , which is defined as one-half the squared-norm of the numerical gradient of the voxels. The prior is calculated so that the mean value of the voxels can be non-zero without penalty. Further, the asymmetric definition of numerical derivative is used,  $\mathbf{dx}_{i,j,k} = \mathbf{x}_{i+1,j,k} - \mathbf{x}_{i,j,k}$ , and similarly for y and z. We use this definition of derivative so that solutions for  $\mathbf{x}$  that have large Nyquist-frequency components are disallowed. Large Nyquist-frequency components would be a problem if the symmetric definition,  $\mathbf{dx}_{i,j,k} = \mathbf{x}_{i+1,j,k} - \mathbf{x}_{i-1,j,k}$ , were used. An example of the solution for a very early frame indicates potentially high degrees of inhomogeneity near the valve of the input tube:

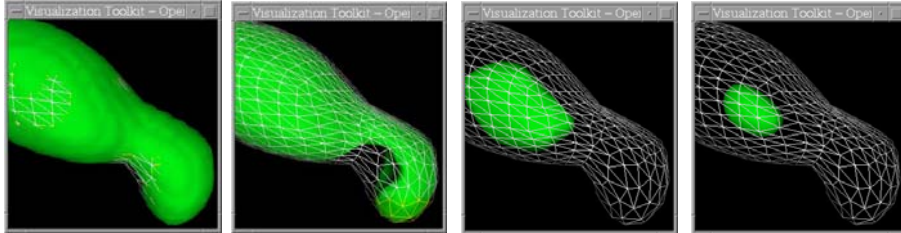


Figure 1. Isocontours of the voxel-to-voxel variation in the estimated radiotracer intensity for frame 46 shows a high degree of inhomogeneity near the input valve. From left to right are isocontours at 12.5%, 25%, 50% and 75% of the maximum intensity, respectively. Wireframe is the estimated surface.

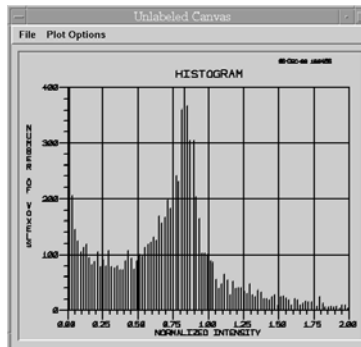


Figure 2. Histogram of radiotracer intensities within volume defined by the surface.

### 2.3 Relaxation of the surface curvature prior at the tract/ventricle join

The prior probability model for the triangulated surface used in our previous work penalizes a discrete approximation to the local curvature at every edge shared by two triangles on the surface in order to enforce smoothness of the estimated surface. Let  $\mathbf{n}_i$  be the normal to the  $i^{\text{th}}$  triangle. We define  $\theta_{ij}$  to be the angle between  $\mathbf{n}_i$  and  $\mathbf{n}_j$ . Then, if  $A_i$  is the area of the  $i^{\text{th}}$  triangle, and  $l_{ij}$  is  $1/3$  the height of the  $i^{\text{th}}$  triangle relative to the edge shared by triangles  $i$  and  $j$ , the curvature prior is defined as

$$\pi(\mathbf{x}) = \sum_i A_i (\sum_j [\tan(\theta_{ij}/2) / l_{ij}]^2), \quad (1)$$

where  $\mathbf{x}$  is the list of  $(x,y,z)$  components for each of the vertices,  $i$  indexes over all triangles on the surface and  $j$  indexes over all triangles that share an edge with the  $i^{\text{th}}$  triangle. The new prior allows for deweighting [4] at edges in an area where high curvature is expected :

$$\pi(\mathbf{x}) = \sum_i A_i (\sum_j W_{ij} [\tan(\theta_{ij}/2) / l_{ij}]^2), \quad (2)$$

where  $W_{ij}$  is 1 if neither of the two vertices that define the edge shared by triangles  $i$  and  $j$  is within the spherical region, and is 0 if either of them is within the spherical region. The effect of this deweighting is illustrated in Fig. 3.

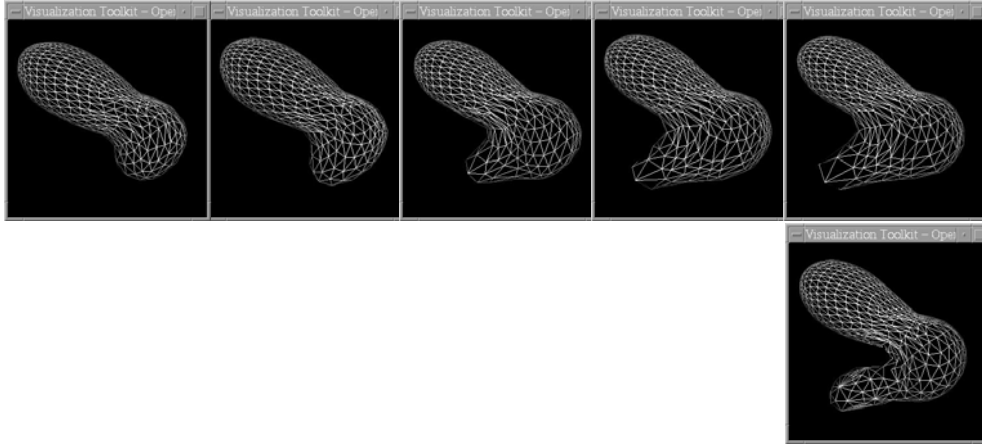


Figure 3. Surface estimates from frames 46, 56, 61, 66 and 71 are shown on top. The input tube is in the top of each image, the ventricle is on the right side, and the output tube is on the bottom. The strong weighting of the prior is encouraging a region of the surface to “grow between” the two tubes on top of the ventricle. On the bottom row is the surface estimate of frame 71 when the curvature prior is deweighted in the region where the input tube and ventricle join.

### 2.3 Estimating the hyperparameters by maximizing the evidence

If one assumes that the posterior is approximately a multi-variate Gaussian, then the evidence can be computed analytically if the determinant of the posterior’s curvature matrix is known. However, since the curvature matrix has dimensions on the order of  $10,000 \times 10,000$ , we need to have a fast method for estimating the determinant for large, sparse matrices. We discuss the application of the method discussed in [7] to our problem, and contrast it to the ad hoc L-curve method.

### Acknowledgments

This work was supported by the U.S. Department of Energy under contract 7405-ENG-36. We thank Irene Pang and Harry Barrett of the University of Arizona for supplying us with the FASTSPECT data and associated system matrix, complete with attenuation correction.